



Published in final edited form as:

*Pain*. 2016 April ; 157(4): 879–891. doi:10.1097/j.pain.0000000000000453.

## Upregulation of the sodium channel $\text{Na}_V\beta 4$ subunit and its contributions to mechanical hypersensitivity and neuronal hyperexcitability in a rat model of radicular pain induced by local DRG inflammation

Wenrui Xie<sup>1</sup>, Zhi-Yong Tan<sup>2</sup>, Cindy Barbosa<sup>2</sup>, Judith A. Strong<sup>1</sup>, Theodore R. Cummins<sup>2</sup>, and Jun-Ming Zhang<sup>1</sup>

<sup>1</sup>Pain Research Center, Department of Anesthesiology, University of Cincinnati College of Medicine, 231 Albert Sabin Way, Cincinnati, OH, 45267, USA

<sup>2</sup>Department of Pharmacology and Toxicology, and Stark Neurosciences Research Institute, Indiana University School of Medicine, Indianapolis, IN 46202, USA

### Abstract

High frequency spontaneous firing in myelinated sensory neurons plays a key role in initiating pain behaviors in several different models, including the radicular pain model in which the rat lumbar dorsal root ganglia (DRG) are locally inflamed. The sodium channel isoform  $\text{Na}_V1.6$  contributes to pain behaviors and spontaneous activity in this model. Among all the isoforms in adult DRG,  $\text{Na}_V1.6$  is the main carrier of TTX-sensitive resurgent Na currents that allow high-frequency firing. Resurgent currents flow after a depolarization or action potential, as a blocking particle exits the pore. In most neurons the regulatory  $\beta 4$  subunit is potentially the endogenous blocker. We used in vivo siRNA mediated knockdown of  $\text{Na}_V\beta 4$  to examine its role in the DRG inflammation model.  $\text{Na}_V\beta 4$  but not control siRNA almost completely blocked mechanical hypersensitivity induced by DRG inflammation. Microelectrode recordings in isolated whole DRGs showed that  $\text{Na}_V\beta 4$  siRNA blocked the inflammation-induced increase in spontaneous activity of A $\beta$  neurons, and reduced repetitive firing and other measures of excitability.  $\text{Na}_V\beta 4$  was preferentially expressed in larger diameter cells; DRG inflammation increased its expression and this was reversed by  $\text{Na}_V\beta 4$  siRNA, based on immunohistochemistry and Western blotting.  $\text{Na}_V\beta 4$  siRNA also reduced immunohistochemical  $\text{Na}_V1.6$  expression. Patch clamp recordings of TTX-sensitive Na currents in acutely cultured medium diameter DRG neurons showed that DRG inflammation increased transient and especially resurgent current; effects blocked by  $\text{Na}_V\beta 4$  siRNA.  $\text{Na}_V\beta 4$  may represent a more specific target for pain conditions that depend on myelinated neurons expressing  $\text{Na}_V1.6$ .

Corresponding author: Jun-Ming Zhang, M.D., M.Sc., Pain Research Center, Department of Anesthesiology, University of Cincinnati, 231 Albert Sabin Way, Cincinnati, OH 45267-0531, Phone 513-558-2427 Fax 513-558-0995, Jun-Ming.Zhang@uc.edu.

The authors declare no competing financial interests.

## Keywords

Nav $\beta$ 4; Scn10a; Scn4b; radicular pain; resurgent current; ectopic activity; Nav1.6; sodium channel

---

## INTRODUCTION

Abnormal spontaneous activity of sensory neurons is an early event in many different preclinical models of neuropathic or inflammatory pain, including the rat radicular pain model produced by local inflammation of one or two lumbar dorsal root ganglion (DRG), and plays a key role in initiating the pain state and later occurring cellular pathological changes [5; 7; 16; 30; 43–45; 47]. In many models, this spontaneous activity consists of high frequency bursting activity that occurs predominantly in myelinated neurons.

Nine different pore-forming  $\alpha$  subunits of voltage-gated sodium channels can mediate the transient, fast-inactivating sodium currents that underlie the action potential in excitable tissues. Normal adult sensory ganglia express 5 of these including Nav1.6 [17]. Many of these isoforms including Nav1.6 can also generate small persistent currents, which can contribute to the membrane potential oscillations that underlie spontaneous activity [1]. Nav1.6 can also give rise to a resurgent sodium current, a brief reopening observed during repolarization or following an action potential [13; 33]. Nav1.6 does not give rise to resurgent currents when expressed in heterologous expression systems, and not all neurons expressing Nav1.6 have resurgent currents [12]. In vivo, each pore-forming  $\alpha$  subunit associates with one or more regulatory  $\beta$  subunits [22]. One of these regulatory proteins, the Nav $\beta$ 4 subunit, has been proposed to confer the ability to generate resurgent currents in neurons. Isoforms and expression systems that lack resurgent currents can produce them when a peptide corresponding to the cytoplasmic terminus of Nav $\beta$ 4 is included in the intracellular solution [20; 29]. This protein has high expression levels in the DRG neurons [53]. Resurgent current allows high frequency repetitive and bursting firing [12; 25; 32], like that observed in DRG neurons after DRG inflammation, spinal nerve ligation, and other pain models.

We previously demonstrated that in vivo knockdown of Nav1.6 strongly reduced mechanical hypersensitivity as well as spontaneous activity and repetitive firing of myelinated neurons induced by local DRG inflammation [46] or spinal nerve ligation [48]. Because the short term knockdown of the channel in these experiments had little effect on single evoked action potentials, these studies provided evidence for an important role of repetitive firing in mediating mechanical hypersensitivity. In this study, we used knockdown of the Nav $\beta$ 4 subunit to test the importance of repetitive firing and resurgent currents in mediating mechanical hypersensitivity and neuronal hyperexcitability induced by local inflammation of the lumbar DRG. This model is intended to mimic conditions such as radicular pain and chemogenic low back pain, in which local inflammation of the DRG may occur, but is also of more general interest because direct effects of inflammatory mediators on sensory neurons play a role in many pain conditions including neuropathic pain [2; 50].

## MATERIALS AND METHODS

### Animals

The experimental protocol was approved by the Institutional Animal Care and Use Committees of the University of Cincinnati and Indiana University School of Medicine. Experiments were conducted in accordance with the National Institutes of Health Guide for the Care and Use of Laboratory Animals. Adult Sprague Dawley rats (Harlan, Indianapolis, USA) of both sexes were used as indicated. Rats were housed two per cage at  $22 \pm 0.5^\circ\text{C}$  with free access to water and food under a controlled diurnal cycle of 14-h light and 10-h dark except as noted.

### Procedure for in vivo injection of siRNA into the DRG

siRNAs directed against rat Nav $\beta$ 4 subunit (Scn4b; gene ID 315611) and nontargeting control were designed by and purchased from Dharmacon/ThermoFisher (Lafayette, CO). The Nav $\beta$ 4-siRNA was siGENOME™ siRNA consisting of a “smartpool” of four different siRNA constructs combined into one reagent. Catalog numbers were M-101002-01 (directed against Nav $\beta$ 4) and D-001210-02 (nontargeting control directed against firefly luciferase, screened to have minimal off-target effects and least 4 mismatches with all known human, mouse and rat genes according to the manufacturer). The sequences for the Nav $\beta$ 4-siRNA were: (construct 1) AAACAACUCUGCUACGAUC, (2) GCAAUACUCAGGCGAGAUG, (3) UCCAAGUGGUUGAUAAAUU and (4) GGAUCGUGAAGAAUGAUAA. 3  $\mu\text{L}$  aliquots containing 80 pmoles of siRNA made up with cationic linear polyethylenimine (PEI)-based transfection reagent (“in vivo JetPEI”, Polyplus Transfection, distributed by WVR Scientific, USA) at a nitrogen/phosphorus ratio of 8 were injected into each L4 and L5 DRG on one side, through a small glass needle (75  $\mu\text{m}$  o.d.) inserted close to the DRG through a small hole cut into the overlying membrane, as previously described [41]. The siRNA was injected just prior to DRG inflammation in experiments using both procedures.

### Surgical procedures for local inflammation of the DRG (LID)

The surgery was performed as previously described [42]. The L5 DRG was inflamed by depositing the immune activator zymosan (2mg/mL, 10 $\mu\text{L}$ , in incomplete Freund’s adjuvant) over the L5 DRG via a small needle inserted into the L5 intervertebral foramen. For animals used for electrophysiological and microscopy experiments the L4 DRG was also inflamed.

### Behavior testing

Mechanical sensitivity was tested by applying a series of von Frey filaments to the heel region of the paws, using the up-and-down method [11]. A cutoff value of 15 grams was assigned to animals that did not respond to the highest filament strength used. A wisp of cotton pulled up from, but still attached to a cotton swab was stroked mediolaterally across the plantar surface of the hindpaws to score the presence or absence of a brisk withdrawal response to a normally innocuous mechanical stimulus (light touch-evoked tactile allodynia). This stimulus does not evoke a response in normal animals. Cold sensitivity was scored as withdrawal responses to a drop of acetone applied to the ventral surface of the hind paw. When observed, responses to acetone or light brush strokes consisted of several rapid flicks

of the paw and/or licking and shaking of the paw; walking movements were not scored as positive responses. Hypersensitivity to thermal (heat) stimuli was not examined because we have previously observed that this behavior is minimally affected by this model [49]. True blinding of the experimenter to the siRNA type injected was found to be difficult due to the large effect size; however a subset of behavioral experiments was conducted with the experimenter blind to the siRNA type, as indicated.

### **Electrophysiology - microelectrode current clamp recordings in whole DRG**

Intracellular recording in current clamp mode was performed at 36 – 37°C using microelectrodes on sensory neurons near the dorsal surface of an acutely isolated whole DRG preparation, as previously described [42]. This preparation allows neurons to be recorded without enzymatic dissociation, with the surrounding satellite glia cells and neighboring neurons intact [34; 54] but does not allow voltage clamp of sodium currents. The DRG was continuously perfused with artificial cerebrospinal fluid (in mM: NaCl 130, KCl 3.5, NaH<sub>2</sub>PO<sub>4</sub> 1.25, NaHCO<sub>3</sub> 24, Dextrose 10, MgCl<sub>2</sub> 1.2, CaCl<sub>2</sub> 1.2, 16 mM HEPES, pH = 7.3, bubbled with 95% O<sub>2</sub>/5% CO<sub>2</sub>). Cells were classified by conduction velocity (stimulation of attached dorsal root) as follows: <1.2 m/s, C; >= 7.5 m/s, A $\beta$ ; between 1.2 and 7.5 m/s, A $\delta$  [35]. Excitability parameters were analyzed as described previously [48]. Briefly, after measurement of any stable spontaneous activity, action potential parameters were measured during the smallest depolarizing current that could evoke an action potential (rheobase). Longer suprathreshold current steps were then applied to determine the maximum number of action potentials that could be evoked, and whether subthreshold membrane oscillations (with characteristic frequencies in the range of 100 – 200 Hz) could be evoked.

### **Electrophysiology - patch clamp recordings of sodium currents**

Rats used for experiments with cultured neurons were housed on a 12:12 light: dark cycle. Adult rat DRG ganglia were dissociated and cultured as previously described [37]. Transient, persistent, and resurgent sodium currents were recorded from neurons after 14 – 28 hours in primary culture. Neurons were dissociated from normal or inflamed (after 3 days) L4 and L5 DRGs or 3 days after siRNA injection and DRG inflammation. The extracellular solution consisted of (in mM): 130 NaCl, 30 TEA chloride, 1 MgCl<sub>2</sub>, 3 KCl, 1 CaCl<sub>2</sub>, 0.05 CdCl<sub>2</sub>, 10 HEPES, and 10 Dextrose, pH 7.3. The pipette solution contained (in mM) 140 CsF, 10 NaCl, 1.1 EGTA, and 10 HEPES, pH 7.3. Resurgent currents were recorded using a two-voltage step protocol. A 20 ms, +30 mV voltage pulse was first used to inactivate transient sodium currents. This was followed by a series of repolarizing pulses to elicit resurgent currents. The repolarizing pulses were 450 ms long, from +5 to –85 mV in 5 mV steps. Resurgent currents were measured as the peak inward current elicited during the repolarizing step. Persistent currents were measured during the last 20 ms of the 450-ms repolarization pulses. Transient current amplitudes were measured using a steady-state inactivation protocol that depolarized the membrane to 0 mV from 500 ms pre-holding at voltage levels from –130 to –5 mV, with an increment of 5 mV. Peak transient currents were measured from the pre-holding level of –110 mV. Peak transient, resurgent and persistent currents were normalized to cell capacitance and expressed as current density values. Voltage dependence of inactivation and activation of the transient current was determined as

in reference [24]; values of  $V_{1/2}$  (voltages at which activation or inactivation was half maximal) are reported. Cells used for recording had diameters of 35 – 45  $\mu\text{m}$ . The median capacitance was 53.8 pF with 25<sup>th</sup> – 75<sup>th</sup> percentile falling in the range 45 – 65 pF.

### Immunostaining in DRG sections

DRG sections were cut at 40  $\mu\text{m}$  on a cryostat after fixation in 4% paraformaldehyde in 0.1M Phosphate Buffer and 4% sucrose. The primary  $\text{Nav}\beta 4$  antibody was from Alomone (Jerusalem, Israel, catalog ASC-044) used at a dilution of 1:150. The secondary antibody conjugated to Alexa Fluor 594 (Invitrogen, Carlsbad, CA) was used at a dilution of 1:1000. Images from multiple sections of each DRG were captured under an Olympus BX61 fluorescent microscope using Slidebook 4.1 imaging acquisition software (Intelligent Imaging Innovation, Denver, CO). To measure the expression of  $\text{Nav}\beta 4$  in the DRG neurons, the summed intensities of the  $\text{Nav}\beta 4$  signal were measured and normalized by the cellular area in each analyzed section to give an intensity ratio. In all immunohistochemical experiments, data from at least four animals were included to control for interanimal variability. For experiments examining effect of  $\text{Nav}\beta 4$  knockdown on  $\text{Nav}1.6$  expression, the procedure was the same except that the polyclonal antibody against  $\text{Nav}1.6$  was used (Alomone; catalog ASC-009, used at 1:100 dilution). For quantification of immunohistochemical data, sections from different experimental groups were examined in a side-by-side protocol with identical display parameters.

### Immunostaining of cultured DRG neurons

To verify knock down of  $\text{Nav}\beta 4$  protein in dissociated DRG cultures under the conditions used for patch clamp measurements of sodium currents, L4/L5 ipsilateral LID DRG ganglia were harvested and cultured from rats injected with non-targeting control or  $\text{Nav}\beta 4$ -siRNA three days after siRNA injection and DRG inflammation. DRG neurons were fixed after 24 hours in culture with 4% paraformaldehyde (0.1 M phosphate buffer, pH 7.4) for 20 min and washed in phosphate buffered saline (PBS) three times. Cells were permeabilized in 1% Triton X-100 in PBS for 20 min at room temperature ( $\sim 22^\circ\text{C}$ ), washed in PBS three times, blocked for 2 h (10% normal goat serum, 0.1% Triton X-100 in PBS) at room temperature and washed an additional three times in PBS. Cells were then incubated with primary antibody against  $\text{Nav}\beta 4$  (#Ab80539, Abcam, Cambridge, MA, USA) diluted 1:500 in blocking solution at 4 degrees overnight. After three washes, cells were incubated with secondary antibody diluted in blocking solution 1:1000 (Alexa Fluor<sup>®</sup> 488 Goat Anti-Rabbit IgG, Molecular Probes, Life Technologies, Grand Island, NY, USA) for 2 h at room temperature. Coverslips were then mounted and imaged with Nikon Eclipse TE2000-E microscope and images were analyzed with NIS Elements Advance (Nikon<sup>®</sup>) software.

### Western blot analysis of $\text{Nav}\beta 4$

DRGs were isolated and homogenized in ice-cold lysis buffer (50 mM Tris pH 7.4, 5 mM EDTA pH 8), 1% Triton X-100 and protease inhibitor cocktail (Complete, EDTA-free, Roche, Life Sciences, Indianapolis IN USA) followed by centrifugation at  $57,000 \times G$  at  $4^\circ\text{C}$  for 60 min. Samples (20  $\mu\text{g}$  of total protein per lane) were subjected to sodium dodecyl sulfate polyacrylamide gel electrophoresis (SDS-PAGE) running in NuPAGE MES SDS running buffer (Invitrogen). Reducing conditions were used to break covalent bonds to the  $\alpha$

subunits [10; 53]. Electrophoresis was followed by electrophoretic transfer to nitrocellulose membrane (Bio-Rad, Hercules, CA, USA) in Tris-glycine-SDS transfer buffer. Nonspecific binding sites were blocked with 5% nonfat dry milk in Tween (Bio-Rad; 0.1%)–phosphate-buffered saline at room temperature for 1 hour. The rabbit antibodies to Na<sub>v</sub>β4 (1:400, Alomone) and to β-Actin (1: 2000, Abcam) were applied to the blot followed by incubation with immunopure peroxidase conjugated goat anti-rabbit IgG (H+L) (1:20,000, Pierce, Rockford, IL). The signal was detected using a ChemiDoc-It system controlled by VisionWorksLS software version 7 (UVP, Upland, CA). After background subtraction, signals in the Na<sub>v</sub>β4 band were normalized to the intensity of the β actin bands.

### Data analysis

Behavioral time course data were analyzed using two-way repeated measures ANOVA with Bonferroni posttest to determine on which days experimental groups differed. For electrophysiological, Western blot, and immunohistochemical data, comparison of values between different experimental groups was done using nonparametric methods for data that did not show a normal distribution based on the D'Agostino and Pearson omnibus normality test. The statistical test used in each case is indicated in the text, or figure legend. Significance was ascribed for  $p < 0.05$ . Levels of significance are indicated by the number of symbols, e.g., \*,  $p = 0.01$  to  $< 0.05$ ; \*\*,  $p = 0.001$  to  $0.01$ ; \*\*\*,  $p < 0.001$ . Data are presented as average  $\pm$  S.E.M.

## RESULTS

### Na<sub>v</sub>β4 knockdown blocks mechanical hypersensitivity in the DRG inflammation model

Previous studies have shown that local inflammation of the L5 DRG causes pronounced mechanical hypersensitivity in the ipsilateral hindpaw as measured by the von Frey test; mechanical allodynia as measured by the withdrawal responses to stroking the paw with a light cotton wisp, a stimulus that never evokes a response in normal animals; and cold allodynia as measured by increased withdrawal to acetone stimuli [42; 49; 52]. These behaviors are observed as early as postoperative day (POD)1; the von Frey response is maintained for at least 4 weeks at which point the other behaviors are beginning to resolve. In the present study, similar results were obtained when nontargeting control siRNA was injected into the L4 and L5 DRG just prior to DRG inflammation (Fig. 1). In this control group, the von Frey threshold differed from baseline on all tested days. However, in animals injected with siRNA directed against Na<sub>v</sub>β4, the ipsilateral mechanical hypersensitivity (von Frey test) was significantly reduced compared to control siRNA on all days tested, and differed from baseline only on POD1. The ipsilateral mechanical allodynia responses (cotton wisp test) were also significantly reduced from the control siRNA group on most days (Fig 1-B), and were significantly different from baseline only on POD1. In contrast, cold allodynia (acetone test) induced by DRG inflammation was not significantly reduced by Na<sub>v</sub>β4 siRNA, either ipsilaterally (Fig 1-C) or contralaterally.

As previously reported in this model [42; 46], contralateral von Frey threshold reductions in the control siRNA group were very modest, with the lowest average value observed on any day being 11 grams. In the Na<sub>v</sub>β4 siRNA group, contralateral thresholds differed from

baseline only on POD1. No animals in either group showed contralateral responses to the mechanical allodynia test on any day.

As shown in Fig. 1, Na $\nu$  $\beta$ 4 siRNA had no effect on baseline behaviors prior to implementation of the pain model; however, the tests used reached cut-off values and would not have detected increased thresholds.

### **Immunohistochemistry and Western blotting confirm Na $\nu$ $\beta$ 4 knockdown by siRNA and upregulation by DRG inflammation**

Immunohistochemical staining for Na $\nu$  $\beta$ 4 was performed in DRG sections from normal animals, and on POD4 after DRG inflammation and injection of nontargeting or Na $\nu$  $\beta$ 4-siRNA. This showed that DRG inflammation upregulated Na $\nu$  $\beta$ 4 and this upregulation was blocked by Na $\nu$  $\beta$ 4-siRNA. This result was confirmed by Western blotting (Fig. 2).

In a separate set of immunohistochemical experiments, examination of sections from both normal and inflamed DRGs showed that Na $\nu$  $\beta$ 4 was not as highly expressed in the cells with the smallest cross-sectional areas. The average cell area of Na $\nu$  $\beta$ 4-positive cells was larger than that of Na $\nu$  $\beta$ 4-negative cells in both conditions, and there were no striking changes in the cell size distribution histograms after DRG inflammation (Fig. 3). The inflammation-induced increase in staining for Na $\nu$  $\beta$ 4 seemed to be primarily due to an increase in the intensity per cell rather than an increase in the percentage of cells expressing Na $\nu$  $\beta$ 4; 62% of all cells scored in normal DRG were Na $\nu$  $\beta$ 4-positive ( $61.5\% \pm 2.2\%$ , based on average values from 4 animals), while 67% of all cells scored in inflamed DRG were Na $\nu$  $\beta$ 4-positive ( $67.7\% \pm 3.4\%$ , based on average values from 4 animals). This increase in percentage was not significant when analyzed based on the average animal values ( $p = 0.17$ , t-test) and could not account for the overall 64% increased average intensity in inflamed compared to normal DRG shown in Fig. 2-D.

Na $\nu$  $\beta$ 4 has also been observed in peripheral axons and nodes. The data in Figure 2 A–D were obtained from cellular regions of the DRG sections, however, we also observed Na $\nu$  $\beta$ 4 in axonal regions, albeit at lower intensities. These regions also showed increased staining after DRG inflammation and reduced staining after Na $\nu$  $\beta$ 4 siRNA injection; examples are shown in Figure, Supplemental Digital Content 1.

The Na $\nu$  $\beta$ 4 siRNA used consisted of a pool of 4 individual constructs. Two separate constructs, used individually, were very effective in reducing mechanical pain, and across the 4 constructs Na $\nu$  $\beta$ 4 knockdown measured with immunohistochemistry correlated well with behavioral effects. These findings (Figure, Supplemental Digital Content 2) argue against the observed effects being due to off-target siRNA effects that are sequence dependent [23].

### **Na $\nu$ $\beta$ 4 knockdown reduces Na $\nu$ 1.6 expression**

The Na $\nu$  $\beta$  subunits can also regulate localization and trafficking of the  $\alpha$  subunits. We therefore examined the effect of Na $\nu$  $\beta$ 4 siRNA on expression of the Na $\nu$ 1.6 subunit in DRG sections. DRG were inflamed and injected with siRNA directed against Na $\nu$  $\beta$ 4 or the nontargeting (n.t.) control construct. Four days later DRGs were fixed and sectioned and

stained for Nav1.6. As shown in the examples in Fig. 4, the expression of Nav1.6 was higher in n.t. siRNA injected DRG (Fig. 4 A–C) than in Navβ4 siRNA injected DRG (Fig. 4 D–F). Summary data from 4 animals per group, 104 sections per animal, showed that Nav1.6 was  $1.6 \pm 0.18$  times higher in n.t. siRNA injected DRG than in Navβ4 siRNA injected DRG (ratio t-test based on animal averages,  $p = 0.002$ ).

### Navβ4 knockdown reduces hyperexcitability induced by DRG inflammation in Aβ sensory neurons

We have previously shown that DRG inflammation leads to marked neuronal hyperexcitability and spontaneous activity of myelinated Aβ neurons in the inflamed DRG, as measured on POD 3–4 in the isolated whole DRG preparation with sharp electrode recording methods. We also showed that injecting siRNA directed against the Nav1.6 sodium channel restored many of these hyperexcitability parameters towards normal values. In this study, we observed a similar reduction of inflammation-induced hyperexcitability of Aβ myelinated cells by injecting Navβ4 siRNA at the time of DRG inflammation (Fig. 5). Spontaneous activity induced by DRG inflammation was restored to normal levels by the Navβ4 siRNA. LID-induced decrease in rheobase was partially normalized by the Navβ4 siRNA (Fig. 5-B); a similar result was observed when spontaneously active cells, with rheobase defined as zero, were excluded from the calculation (data not shown). The observed changes in rheobase did not reflect changes in input resistance ( $16.3 \pm 0.1$ ,  $16.0 \pm 0.7$ , and  $17.0 \pm 0.7$  MΩ in normal + n.t. siRNA, LID + Navβ4 siRNA, and LID + n.t. siRNA, respectively; no significant differences between groups per Kruskal-Wallis test with Dunn's post-test). DRG inflammation caused a small resting membrane depolarization (from  $-66.2 \pm 0.5$  to  $-62.1 \pm 0.7$  mV) that was partially normalized by Navβ4 siRNA (to  $-64.1 \pm 0.5$  mV; Fig. 5-D). Action potential duration was slightly increased by LID but not affected by Navβ4 siRNA (Fig. 5-C). Action potential threshold did not differ between the three groups (data not shown). Parameters particularly associated with resurgent and persistent currents, such as the ability to fire repetitively or show subthreshold membrane oscillations in response to long suprathreshold current injections, were also increased by DRG inflammation and largely normalized by Navβ4 knockdown (Fig. 5-E and 5-F).

The number of Aδ cells observed in these experiments was relatively small (26 in the control group, only 8 in the LID + nontargeting siRNA group, and 45 in the LID + Navβ4 siRNA group); few significant differences in the electrophysiological parameters were observed and none of the cells showed spontaneous activity (data not shown).

In contrast to the results with Aβ cells, electrophysiological parameters of C cells were much less affected by DRG inflammation or Navβ4 siRNA (Fig. 6). Spontaneous activity was low or zero in all groups and there were no significant differences between groups. Rheobase (Fig. 6-B), membrane potential (Fig. 6-D), threshold (data not shown), and ability to fire repetitively (Fig. 6-E) were not affected by DRG inflammation or by Navβ4 siRNA. The action potential width was increased by DRG inflammation but there was no effect of Navβ4 siRNA (Fig. 6-C). Somewhat paradoxically, the percentage of C cells in which suprathreshold currents could induce membrane potential oscillations was higher after Navβ4 knockdown; a similar effect was previously reported after Nav1.6 knockdown [46].

### **DRG inflammation increases transient and resurgent TTX-sensitive Na currents in medium diameter cells in vitro**

We next examined the effects of DRG inflammation and Nav $\beta$ 4 knockdown on resurgent sodium currents, since these currents are thought to facilitate high frequency repetitive firing. Transient, resurgent, and persistent Na currents were recorded in acutely isolated, medium diameter (35 to 45  $\mu$ m) neurons from DRGs from sham operated animals or DRGs isolated 3 days after DRG inflammation. To ensure a better quality of recording, medium-sized (35 to 45  $\mu$ m) but not large-sized (more than 45  $\mu$ m) DRG neurons were chosen to ensure a better voltage control; in addition, our previous microelectrode studies have shown that spontaneous activity occurs primarily in A $\beta$  cells towards the smaller end of the diameter distribution [42], and previous patch clamp studies showed that medium diameter neurons have a high likelihood of expressing Nav1.6, the main carrier of TTX-sensitive resurgent current in DRG neurons [13]. Cells were classified as having predominantly TTX-sensitive current (based on fast current kinetics and a single component in steady-state inactivation curves) or mixed TTX-sensitive and TTX-resistant currents, as previously described [14; 19]. Because the microelectrode recordings show that spontaneous activity and hyperexcitability are predominantly observed in A $\beta$  cells and are TTX-sensitive [42], we focused on the subset of cells with predominantly TTX-sensitive currents. In addition, cells with predominantly TTX-sensitive current have previously been observed to be the ones to express TTX-sensitive resurgent currents (Tan et al., 2014). Excluding cells with mixed TTX-R and TTX-S Na currents also most likely excluded most cells with A $\delta$  conduction velocities in vivo [18], even though those would otherwise be expected to be enriched in the size range examined. In those cells with predominantly TTX-sensitive current, both peak transient and peak resurgent current densities were increased by DRG inflammation (Fig. 7). Resurgent current was also preferentially increased: the ratio of resurgent to transient current increased from  $0.034 \pm 0.002$  in control cells to  $0.041 \pm 0.002$  in inflamed cells ( $p = 0.02$ , Mann-Whitney test). Persistent current density was  $4.0 \pm 0.63$  in control cells vs.  $5.7 \pm 0.61$  pA/pF in cells from inflamed DRG, a difference that did not quite reach significance ( $p = 0.055$ , Mann-Whitney test). The ratio of persistent to transient current was  $0.003 \pm 0.0005$  in control cells and  $0.003 \pm 0.0004$  in cells from inflamed DRG ( $p = 0.46$ , t-test).

Cells from inflamed DRG also had a negative shift in the voltage dependence of activation of the transient current ( $V_{1/2}$  of  $-46.4 \pm 0.9$  mV compared to  $-41.8 \pm 1.6$  mV in control cells;  $p = 0.03$ , t-test). There was also a small shift in steady-state inactivation ( $\sim 2.5$  mV) which may not have had a major impact on channel availability ( $V_{1/2} = -57.3 \pm 0.8$  in LID cells vs.  $-59.9 \pm 0.8$  in control cells,  $p = 0.04$ , t test).

### **Nav $\beta$ 4 knockdown in vivo preferentially reduces TTX-sensitive persistent and resurgent currents in medium diameter neurons cultured from inflamed DRG**

In a separate set of experiments, transient, resurgent, and persistent Na currents were recorded in acutely isolated, medium (35 to 45  $\mu$ m) diameter neurons from cultured DRGs isolated 3 days after in vivo DRG inflammation and injection of either nontargeting control or Nav $\beta$ 4 siRNA. Cells having only TTX-sensitive currents were chosen to study based on the same criteria and reasons described above. In those cells, densities of both resurgent currents and persistent currents were reduced by the Nav $\beta$ 4 siRNA (Fig. 8). The ratio of

resurgent to transient current was also significantly lower in  $\text{Na}_V\beta 4$  siRNA treated cells ( $0.048 \pm 0.003$  with n.t. siRNA vs.  $0.033 \pm 0.002$  with  $\text{Na}_V\beta 4$  siRNA,  $p = 0.0003$ , Mann-Whitney test). In addition, the ratio of persistent to transient current was lower ( $0.0034 \pm 0.0003$  in n.t. siRNA group vs.  $0.0023 \pm 0.0003$ ,  $p = 0.0005$ , Mann-Whitney test).

$\text{Na}_V\beta 4$  knockdown also resulted in a depolarizing shift in the voltage dependence of activation of the transient current (from  $V_{1/2}$  of  $-48.2 \pm 1.9$  to  $-42.4 \pm 1.2$  mV,  $p = 0.01$ , t-test). There was no significant difference between the 2 groups in the voltage dependence of inactivation.

Knockdown of  $\text{Na}_V\beta 4$  under the experimental conditions used for the patch clamp recordings was confirmed with immunostaining of cultured neurons (Fig. 9). To parallel the protocol used for the patch clamp experiments, siRNA (nontargeting or  $\text{Na}_V\beta 4$  directed) was injected in vivo at the time of DRG inflammation; DRGs were isolated and dissociated 3 days later, and cultured cells were fixed and stained after 24 hours in culture.

## DISCUSSION

We found that knockdown of  $\text{Na}_V\beta 4$  via intraganglionic siRNA injection almost completely prevented the development of mechanical hypersensitivity after local inflammation of the DRG, that both  $\text{Na}_V 1.6$  and  $\text{Na}_V\beta 4$  subunits are upregulated on POD 3 – 4 in this model at the protein level ([46] and Fig. 2), and that DRG inflammation increased TTX-sensitive resurgent and transient currents in medium diameter cells in vitro.

$\text{Na}_V\beta 4$  can be expressed in nonneuronal cells and have effects independent of the  $\text{Na}_V\alpha$  subunits [9; 31]. However, our immunohistochemical data in DRG sections and cultured neurons show that the majority of neurons express  $\text{Na}_V\beta 4$ . The behavioral effects of  $\text{Na}_V\beta 4$  knockdown in the lumbar DRG are also strikingly similar to those of  $\text{Na}_V 1.6$  knockdown [46], differing only on POD1 when the  $\text{Na}_V\beta 4$  knockdown effect on von Frey responding is only partial but the  $\text{Na}_V 1.6$  knockdown effect is complete. Both  $\text{Na}_V\beta 4$  and  $\text{Na}_V 1.6$  knockdown block mechanical pain behaviors for the duration of the experiment (at least 4 weeks). As it is unlikely that the single siRNA injection was effective for this long, we interpret this to mean that an early period of spontaneous activity is required to initiate long-lasting pain behaviors, consistent with our other studies in this and other rat pain models [42; 45; 48].

We demonstrated that mechanical hypersensitivity induced by DRG inflammation was ameliorated by  $\text{Na}_V\beta 4$  knockdown; however the effects on pain behaviors requiring higher brain centers remain to be determined. We have previously shown that the DRG inflammation model causes a naproxen-sensitive decrease in a more complex behavior (rearing) [42]. Interestingly, a recent study showed that many human patients with radicular (but not axial) low back pain also exhibited hypersensitivity to von Frey and cold stimuli in the leg and foot [15].

We propose two mechanisms that may contribute to the observed behavioral and electrophysiological effects of  $\text{Na}_V\beta 4$  knockdown and reduction of spontaneous activity in myelinated A $\beta$  cells: (1) reduction of  $\text{Na}_V 1.6$  expression; and (2) reduction of resurgent and



Changes in the voltage-dependence of sodium channel activation and inactivation can also contribute to altered excitability. Previous studies examining the impact of  $\text{Na}_V\beta 4$  on recombinant  $\text{Na}_V 1.6$  channels expressed in heterologous cells such as HEK293 cells indicate that  $\text{Na}_V\beta 4$  can induce negative shifts in the voltage-dependence of activation (almost  $-10$  mV) and, to a lesser extent, steady-state inactivation[55]. We observed a hyperpolarizing shift in activation with inflammation of the DRG; this is likely to enhance spontaneous firing in sensory neurons.  $\text{Na}_V\beta 4$  knockdown also induced a  $+6$  mV shift in the voltage-dependence of activation, supporting the notion that  $\text{Na}_V\beta 4$  subunits modify  $\text{Na}_V 1.6$  voltage-dependence of activation.

Our results confirm and extend previous work showing that  $\text{Na}_V\beta 4$  is primarily expressed in larger sensory neurons and that it plays a key role in mediating resurgent currents in inflamed, hypersensitive sensory neurons [4; 26; 53].

In this study the patch clamp experiments on Na currents were conducted on medium diameter neurons expressing only TTX-sensitive sodium currents. This focus was dictated by our previous work showing that spontaneous activity in this model is TTX-sensitive and largely observed in cells at the smaller end of the size range for  $\text{A}\beta$  neurons. By excluding cells expressing both TTX-resistant and TTX-sensitive currents, we most likely avoided studying many  $\text{A}\delta$  neurons [18]. TTX-resistant resurgent Na currents mediated by  $\text{Na}_V 1.8$  and enhanced by the  $\text{Na}_V\beta 4$  cytoplasmic terminus have also been observed in DRG neurons [37]. These resurgent currents activate over an order of magnitude more slowly than those mediated by  $\text{Na}_V 1.6$ ; e.g. at  $-20$  mV the times to peak are 130 msec compared to 3.5 msec. Thus it is not clear that these currents could facilitate the high frequency firing observed in our model, in which the interspike interval is commonly less than 10 msec.  $\text{Na}_V 1.8$  has recently been found to be upregulated in myelinated  $\text{A}\beta$  neurons by peripheral inflammation (CFA paw injection) [6] and therefore a possible role of  $\text{Na}_V 1.8$  in our model remains to be investigated. Arguing against it playing a predominant role in our model are the observations that peripheral inflammation with CFA and local DRG inflammation yield DRG gene expression changes with almost no overlap [36], and the complete elimination of both pain behaviors and spontaneous activity by  $\text{Na}_V 1.6$  knockdown [46]. In addition our preliminary experiments using protocols similar to this study showed no effect of  $\text{Na}_V 1.8$  knockdown on pain behaviors induced by DRG inflammation through POD 4.

## Conclusions

Although  $\text{Na}_V 1.6$  has not generally been considered a good therapeutic target for pain, due to its widespread distribution and key role in the node of Ranvier, our results suggest that targeting the persistent and resurgent currents generated by this channel (which often depend on  $\text{Na}_V\beta 4$ ) might be a promising approach. Resurgent and persistent currents share many common regulators, including the  $\text{Na}_V\beta 4$  subunit [3], several drugs [38], and an epilepsy model [21]. Pharmacological separation of persistent from resurgent currents may prove difficult, but if blocking abnormal spontaneous activity is to be considered a therapeutic goal, agents that block both may be quite useful. Some drugs have been shown to preferentially target persistent and resurgent currents over the transient current that underlies the action potential upstroke [27; 38; 40; 42; 51]. In this vein it is interesting that a toxin that

enhances resurgent and persistent currents in large diameter DRG neurons in mice causes acute pain and itch when injected into humans, effects that are mediated by myelinated fibers [26]. Increased persistent and resurgent Na currents have also been implicated in a mouse model of epilepsy [21]. In humans some mutations that increase resurgent currents have been associated with pain [24; 39]. Na channels have long been a primary therapeutic target for pain; we suggest that the regulatory  $\beta$  subunits may provide a more specific therapeutic target than the pore-forming  $\alpha$  subunits, particularly for pain conditions mediated by the widely expressed Nav1.6 isoform.

## Supplementary Material

Refer to Web version on PubMed Central for supplementary material.

## Acknowledgments

Supported in part by National Institutes of Health grants NS045594 and NS055860 to J.-M. Z, NS053422 to T.R.C. and NRSA F31 NS090837 to C.B.

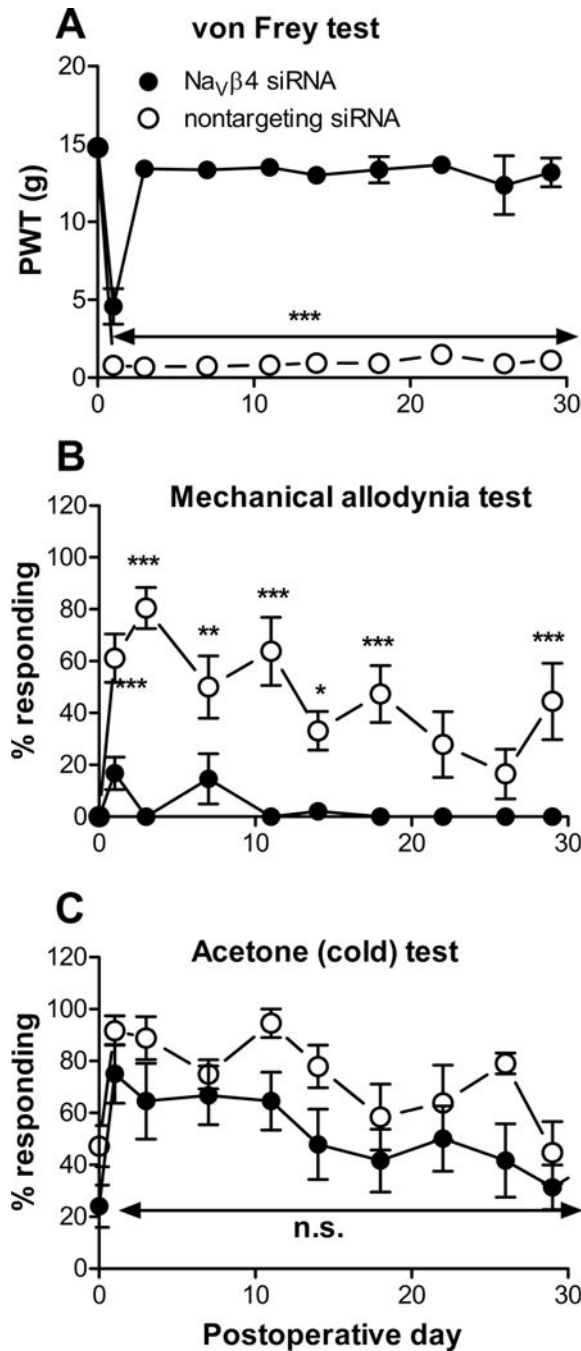
## References

1. Amir R, Liu CN, Kocsis JD, Devor M. Oscillatory mechanism in primary sensory neurones. *Brain*. 2002; 125(Pt 2):421–435. [PubMed: 11844741]
2. Austin PJ, Moalem-Taylor G. The neuro-immune balance in neuropathic pain: Involvement of inflammatory immune cells, immune-like glial cells and cytokines. *J Neuroimmunol*. 2010; 229(1–2):26–50. [PubMed: 20870295]
3. Bant JS, Raman IM. Control of transient, resurgent, and persistent current by open-channel block by Na channel beta4 in cultured cerebellar granule neurons. *Proc Natl Acad Sci U S A*. 2010; 107(27):12357–12362. [PubMed: 20566860]
4. Barbosa C, Tan ZY, Wang R, Xie W, Strong JA, Patel RR, Vasko MR, Zhang J-M, Cummins TR. Nav $\beta$ 4 regulates fast resurgent sodium currents and excitability in sensory neurons. *Molecular Pain*. 2015; 11(1):60. [PubMed: 26408173]
5. Bedi SS, Yang Q, Crook RJ, Du J, Wu Z, Fishman HM, Grill RJ, Carlton SM, Walters ET. Chronic spontaneous activity generated in the somata of primary nociceptors is associated with pain-related behavior after spinal cord injury. *J Neurosci*. 2010; 30(44):14870–14882. [PubMed: 21048146]
6. Belkouch M, Dansereau MA, Tetreault P, Biet M, Beaudet N, Dumaine R, Chraïbi A, Melik-Parsadaniantz S, Sarret P. Functional up-regulation of Nav1.8 sodium channel in Abeta afferent fibers subjected to chronic peripheral inflammation. *J Neuroinflammation*. 2014; 11:45. [PubMed: 24606981]
7. Berger JV, Knaepen L, Janssen SP, Jaken RJ, Marcus MA, Joosten EA, Deumens R. Cellular and molecular insights into neuropathy-induced pain hypersensitivity for mechanism-based treatment approaches. *Brain Res Rev*. 2011; 67(1–2):282–310. [PubMed: 21440003]
8. Black JA, Renganathan M, Waxman SG. Sodium channel Na(v)1.6 is expressed along nonmyelinated axons and it contributes to conduction. *Brain Res Mol Brain Res*. 2002; 105(1–2):19–28. [PubMed: 12399104]
9. Brackenbury WJ, Isom LL. Na Channel beta Subunits: Overachievers of the Ion Channel Family. *Front Pharmacol*. 2011; 2:53. [PubMed: 22007171]
10. Buffington SA, Rasband MN. Na<sup>+</sup> channel-dependent recruitment of Nav $\beta$ 4 to axon initial segments and nodes of Ranvier. *J Neurosci*. 2013; 33(14):6191–6202. [PubMed: 23554500]
11. Chaplan SR, Bach FW, Pogrel JW, Chung JM, Yaksh TL. Quantitative assessment of tactile allodynia in the rat paw. *Journal of Neuroscience Methods*. 1994; 53(1):55–63. [PubMed: 7990513]

12. Cruz JS, Silva DF, Ribeiro LA, Araujo IG, Magalhaes N, Medeiros A, Freitas C, Araujo IC, Oliveira FA. Resurgent Na<sup>+</sup> current: a new avenue to neuronal excitability control. *Life Sci.* 2011; 89(15–16):564–569. [PubMed: 21683085]
13. Cummins TR, Dib-Hajj SD, Herzog RI, Waxman SG. Nav1.6 channels generate resurgent sodium currents in spinal sensory neurons. *FEBS Lett.* 2005; 579(10):2166–2170. [PubMed: 15811336]
14. Cummins TR, Waxman SG. Downregulation of tetrodotoxin-resistant sodium currents and upregulation of a rapidly repriming tetrodotoxin-sensitive sodium current in small spinal sensory neurons after nerve injury. *J Neurosci.* 1997; 17(10):3503–3514. [PubMed: 9133375]
15. Defrin R, Devor M, Brill S. Tactile allodynia in patients with lumbar radicular pain (sciatica). *Pain.* 2014; 155(12):2551–2559. [PubMed: 25242568]
16. Devor M. Ectopic discharge in A $\beta$  afferents as a source of neuropathic pain. *Exp Brain Res.* 2009; 196(1):115–128. [PubMed: 19242687]
17. Dib-Hajj SD, Cummins TR, Black JA, Waxman SG. Sodium channels in normal and pathological pain. *Annu Rev Neurosci.* 2010; 33:325–347. [PubMed: 20367448]
18. Djouhri L, Fang X, Okuse K, Wood JN, Berry CM, Lawson SN. The TTX-resistant sodium channel Nav1.8 (SNS/PN3): expression and correlation with membrane properties in rat nociceptive primary afferent neurons. *J Physiol.* 2003; 550(Pt 3):739–752. [PubMed: 12794175]
19. Everill B, Cummins TR, Waxman SG, Kocsis JD. Sodium currents of large (A $\beta$ -type) adult cutaneous afferent dorsal root ganglion neurons display rapid recovery from inactivation before and after axotomy. *Neuroscience.* 2001; 106(1):161–169. [PubMed: 11564426]
20. Grieco TM, Malhotra JD, Chen C, Isom LL, Raman IM. Open-channel block by the cytoplasmic tail of sodium channel beta4 as a mechanism for resurgent sodium current. *Neuron.* 2005; 45(2): 233–244. [PubMed: 15664175]
21. Hargus NJ, Merrick EC, Nigam A, Kalmar CL, Baheti AR, Bertram EH 3rd, Patel MK. Temporal lobe epilepsy induces intrinsic alterations in Na channel gating in layer II medial entorhinal cortex neurons. *Neurobiol Dis.* 2011; 41(2):361–376. [PubMed: 20946956]
22. Isom LL. I. Cellular and molecular biology of sodium channel beta-subunits: therapeutic implications for pain? *Am J Physiol Gastrointest Liver Physiol.* 2000; 278(3):G349–353. [PubMed: 10712253]
23. Jackson AL, Linsley PS. Recognizing and avoiding siRNA off-target effects for target identification and therapeutic application. *Nat Rev Drug Discov.* 2010; 9(1):57–67. [PubMed: 20043028]
24. Jarecki BW, Piekarz AD, Jackson JO 2nd, Cummins TR. Human voltage-gated sodium channel mutations that cause inherited neuronal and muscle channelopathies increase resurgent sodium currents. *J Clin Invest.* 2010; 120(1):369–378. [PubMed: 20038812]
25. Khaliq ZM, Gouwens NW, Raman IM. The contribution of resurgent sodium current to high-frequency firing in Purkinje neurons: an experimental and modeling study. *J Neurosci.* 2003; 23(12):4899–4912. [PubMed: 12832512]
26. Klinger AB, Eberhardt M, Link AS, Namer B, Kutsche LK, Schuy ET, Sittl R, Hoffmann T, Alzheimer C, Huth T, Carr RW, Lampert A. Sea-anemone toxin ATX-II elicits A-fiber-dependent pain and enhances resurgent and persistent sodium currents in large sensory neurons. *Mol Pain.* 2012; 8:69. [PubMed: 22978421]
27. Kononenko NI, Shao LR, Dudek FE. Riluzole-sensitive slowly inactivating sodium current in rat suprachiasmatic nucleus neurons. *J Neurophysiol.* 2004; 91(2):710–718. [PubMed: 14573554]
28. Krzemien DM, Schaller KL, Levinson SR, Caldwell JH. Immunolocalization of sodium channel isoform NaCh6 in the nervous system. *J Comp Neurol.* 2000; 420(1):70–83. [PubMed: 10745220]
29. Lewis AH, Raman IM. Resurgent current of voltage-gated Na<sup>(+)</sup> channels. *J Physiol.* 2014; 592(Pt 22):4825–4838. [PubMed: 25172941]
30. Nieto FR, Cobos EJ, Tejada MA, Sanchez-Fernandez C, Gonzalez-Cano R, Cendan CM. Tetrodotoxin (TTX) as a therapeutic agent for pain. *Mar Drugs.* 2012; 10(2):281–305. [PubMed: 22412801]
31. Patino GA, Isom LL. Electrophysiology and beyond: multiple roles of Na<sup>+</sup> channel beta subunits in development and disease. *Neurosci Lett.* 2010; 486(2):53–59. [PubMed: 20600605]

32. Raman IM, Bean BP. Resurgent sodium current and action potential formation in dissociated cerebellar Purkinje neurons. *J Neurosci*. 1997; 17(12):4517–4526. [PubMed: 9169512]
33. Raman IM, Sprunger LK, Meisler MH, Bean BP. Altered subthreshold sodium currents and disrupted firing patterns in Purkinje neurons of Scn8a mutant mice. *Neuron*. 1997; 19(4):881–891. [PubMed: 9354334]
34. Song XJ, Hu SJ, Greenquist KW, Zhang J-M, LaMotte RH. Mechanical and thermal hyperalgesia and ectopic neuronal discharge after chronic compression of dorsal root ganglia. *Journal of Neurophysiology*. 1999; 82(6):3347–3358. [PubMed: 10601466]
35. Stebbing MJ, Eschenfelder S, Habler HJ, Acosta MC, Janig W, McLachlan EM. Changes in the action potential in sensory neurones after peripheral axotomy in vivo. *Neuroreport*. 1999; 10(2): 201–206. [PubMed: 10203309]
36. Strong JA, Xie W, Coyle DE, Zhang JM. Microarray analysis of rat sensory ganglia after local inflammation implicates novel cytokines in pain. *PLoS One*. 2012; 7(7):e40779. [PubMed: 22815815]
37. Tan ZY, Piekarz AD, Priest BT, Knopp KL, Krajewski JL, McDermott JS, Nisenbaum ES, Cummins TR. Tetrodotoxin-resistant sodium channels in sensory neurons generate slow resurgent currents that are enhanced by inflammatory mediators. *J Neurosci*. 2014; 34(21):7190–7197. [PubMed: 24849353]
38. Theile JW, Cummins TR. Inhibition of Navbeta4 peptide-mediated resurgent sodium currents in Nav1.7 channels by carbamazepine, riluzole, and anandamide. *Mol Pharmacol*. 2011; 80(4):724–734. [PubMed: 21788423]
39. Theile JW, Jarecki BW, Piekarz AD, Cummins TR. Nav1.7 mutations associated with paroxysmal extreme pain disorder, but not erythromelalgia, enhance Navbeta4 peptide-mediated resurgent sodium currents. *J Physiol*. 2010; 589(Pt 3):597–608. [PubMed: 21115638]
40. Urbani A, Belluzzi O. Riluzole inhibits the persistent sodium current in mammalian CNS neurons. *Eur J Neurosci*. 2000; 12(10):3567–3574. [PubMed: 11029626]
41. Xie W, Strong JA, Kays J, Nicol GD, Zhang JM. Knockdown of the sphingosine-1-phosphate receptor S1PR1 reduces pain behaviors induced by local inflammation of the rat sensory ganglion. *Neurosci Lett*. 2012; 515(1):61–65. [PubMed: 22445889]
42. Xie W, Strong JA, Kim D, Shahrestani S, Zhang JM. Bursting activity in myelinated sensory neurons plays a key role in pain behavior induced by localized inflammation of the rat sensory ganglion. *Neuroscience*. 2012; 206:212–223. [PubMed: 22265726]
43. Xie W, Strong JA, Li H, Zhang J-M. Sympathetic sprouting near sensory neurons after nerve injury occurs preferentially on spontaneously active cells and is reduced by early nerve block. *J Neurophysiol*. 2007; 97(1):492–502. [PubMed: 17065247]
44. Xie W, Strong JA, Mao J, Zhang JM. Highly localized interactions between sensory neurons and sprouting sympathetic fibers observed in a transgenic tyrosine hydroxylase reporter mouse. *Mol Pain*. 2011; 7:53. [PubMed: 21794129]
45. Xie W, Strong JA, Meij JT, Zhang J-M, Yu L. Neuropathic pain: Early spontaneous afferent activity is the trigger. *Pain*. 2005; 116(3):243–256. [PubMed: 15964687]
46. Xie W, Strong JA, Ye L, Mao JX, Zhang J-M. Knockdown of sodium channel Nav1.6 blocks mechanical pain and abnormal bursting activity of afferent neurons in inflamed sensory ganglia. *Pain*. 2013; 154:1170–1180. [PubMed: 23622763]
47. Xie W, Strong JA, Zhang JM. Early blockade of injured primary sensory afferents reduces glial cell activation in two rat neuropathic pain models. *Neuroscience*. 2009; 160(4):847–857. [PubMed: 19303429]
48. Xie W, Strong JA, Zhang JM. Local knockdown of the Nav1.6 sodium channel reduces pain behaviors, sensory neuron excitability, and sympathetic sprouting in rat models of neuropathic pain. *Neuroscience*. 2015; 16:291–317.
49. Xie WR, Deng H, Li H, Bowen TL, Strong JA, Zhang J-M. Robust increase of cutaneous sensitivity, cytokine production and sympathetic sprouting in rats with localized inflammatory irritation of the spinal ganglia. *Neuroscience*. 2006; 142(3):809–822. [PubMed: 16887276]
50. Xu Q, Yaksh TL. A brief comparison of the pathophysiology of inflammatory versus neuropathic pain. *Curr Opin Anaesthesiol*. 2011; 24(4):400–407. [PubMed: 21659872]

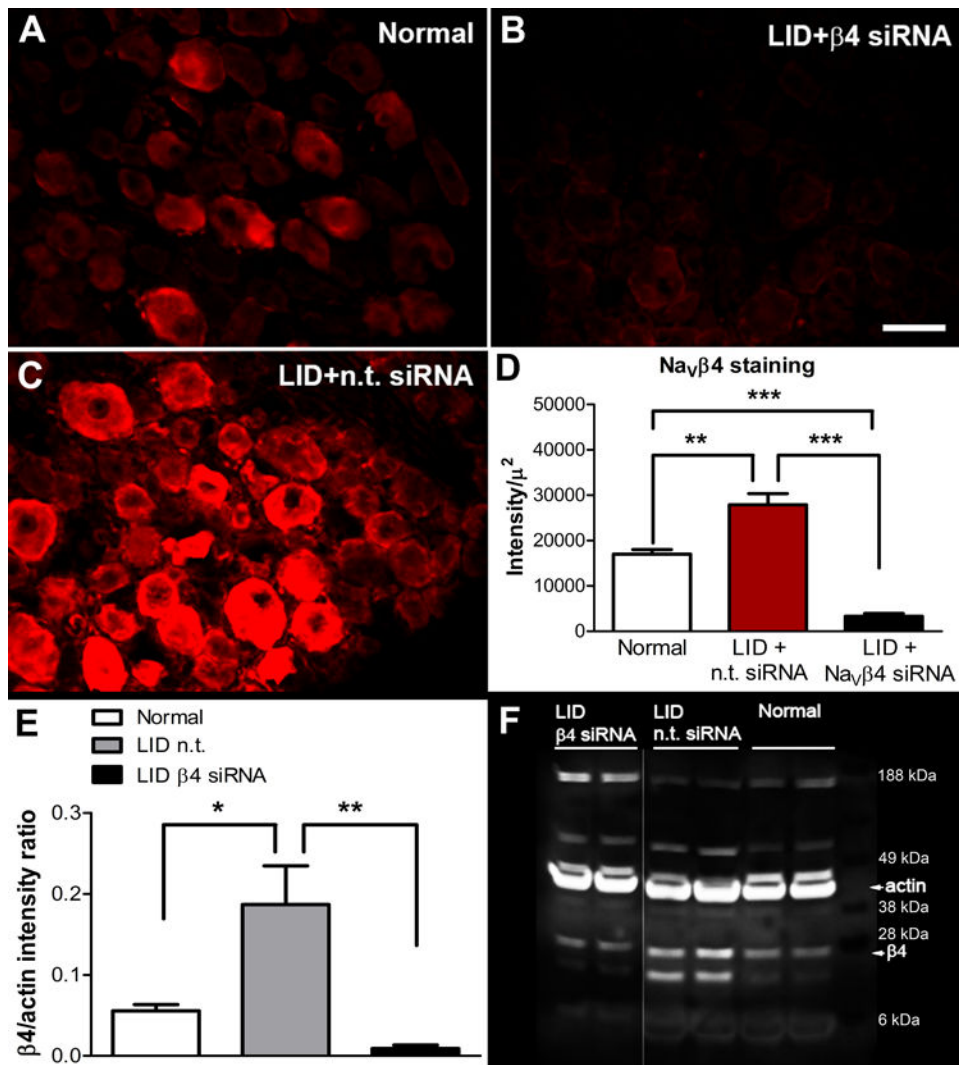
51. Yang RH, Wang WT, Chen JY, Xie RG, Hu SJ. Gabapentin selectively reduces persistent sodium current in injured type-A dorsal root ganglion neurons. *Pain*. 2009; 143(1–2):48–55. [PubMed: 19269740]
52. Ye L, Xie W, Strong JA, Zhang JM. Blocking the Mineralocorticoid Receptor Improves Effectiveness of Steroid Treatment for Low Back Pain in Rats. *Anesthesiology*. 2014
53. Yu FH, Westenbroek RE, Silos-Santiago I, McCormick KA, Lawson D, Ge P, Ferriera H, Lilly J, DiStefano PS, Catterall WA, Scheuer T, Curtis R. Sodium channel beta4, a new disulfide-linked auxiliary subunit with similarity to beta2. *J Neurosci*. 2003; 23(20):7577–7585. [PubMed: 12930796]
54. Zhang J-M, Song XJ, LaMotte RH. Enhanced excitability of sensory neurons in rats with cutaneous hyperalgesia produced by chronic compression of the dorsal root ganglion. *Journal of Neurophysiology*. 1999; 82(6):3359–3366. [PubMed: 10601467]
55. Zhao J, O’Leary ME, Chahine M. Regulation of Nav1.6 and Nav1.8 peripheral nerve Na<sup>+</sup> channels by auxiliary beta-subunits. *J Neurophysiol*. 2011; 106(2):608–619. [PubMed: 21562192]



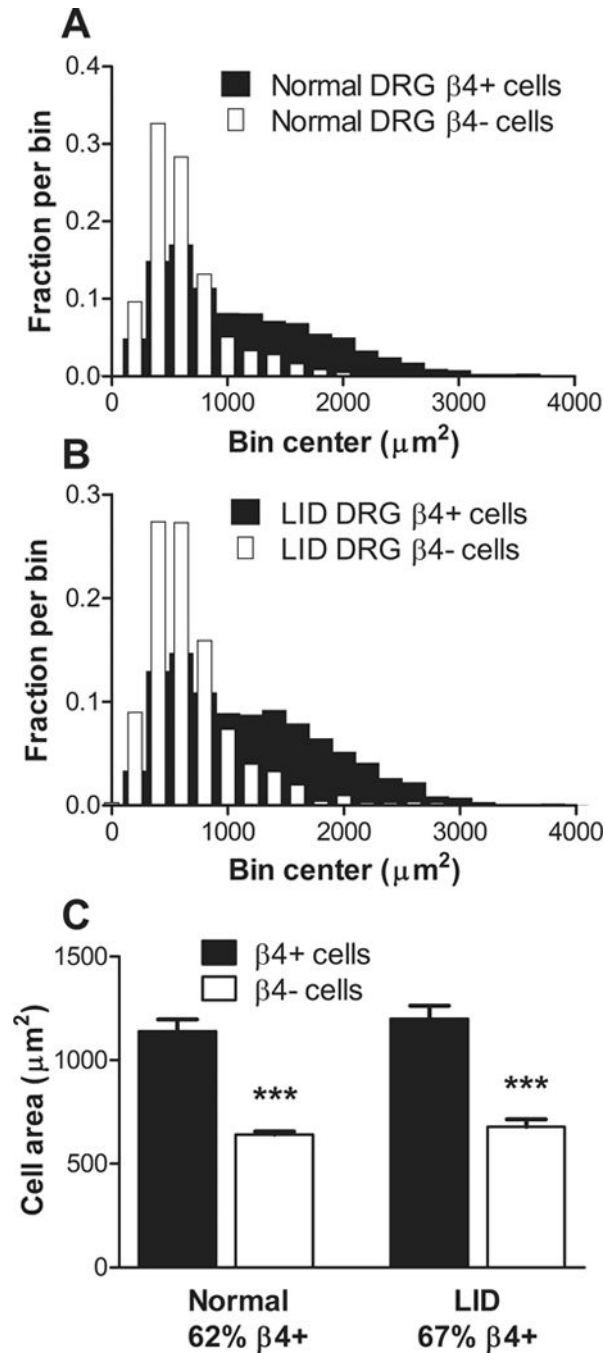
**Figure 1.**

Effects of  $Na_V\beta_4$  knockdown on pain behaviors elicited by local inflammation of the L5 DRG. Baseline measurements plotted on postoperative day (POD) 0 are the average of 2 measurements made 3 – 5 days prior to inflammation of the L5 DRG and injection of siRNA directed against  $Na_V\beta_4$  or nontargeting (n.t.) control siRNA on POD0. A: Mechanical threshold measured by the von Frey test was significantly reduced for the duration of the experiment in the n.t. injected animals. In  $Na_V\beta_4$  siRNA injected animals the threshold differed from the n.t. animals on all days except baseline. B: Mechanical allodynia,

measured as withdrawal to stroking the paw with a fine cotton wisp, was never observed prior to DRG inflammation (average baseline plotted on POD0), was increased by DRG inflammation in n.t. siRNA injected animals, and was significantly less on most days in Nav $\beta$ 4 siRNA injected animals. In Nav $\beta$ 4 siRNA injected animals the decreased threshold was significantly different from baseline only on POD1; in n.t injected animals the decreased threshold differed significantly from baseline on all POD except POD 14 and 22. C. Cold allodynia, measured as withdrawal to a drop of acetone placed on the paw, was increased by DRG inflammation but not significantly affected by Nav $\beta$ 4 siRNA. N = 6 n.t. and 8 Nav $\beta$ 4 siRNA injected male rats. \*, p< 0.05, \*\*, p<0.01, \*\*\*, p<0.001, significant difference between the two groups (two-way repeated measures ANOVA with Bonferroni posttest). Differences from baseline on later POD within each group discussed above were tested using one-way ANOVA with Dunnett's posttest. The data presented in the figure were not obtained with blinding of the experimenter; however, the findings about the initial time course of pain behaviors were confirmed in a separate experiment in which the experimenter was blinded to the siRNA status of the animals, n = 4 per group, data not shown.



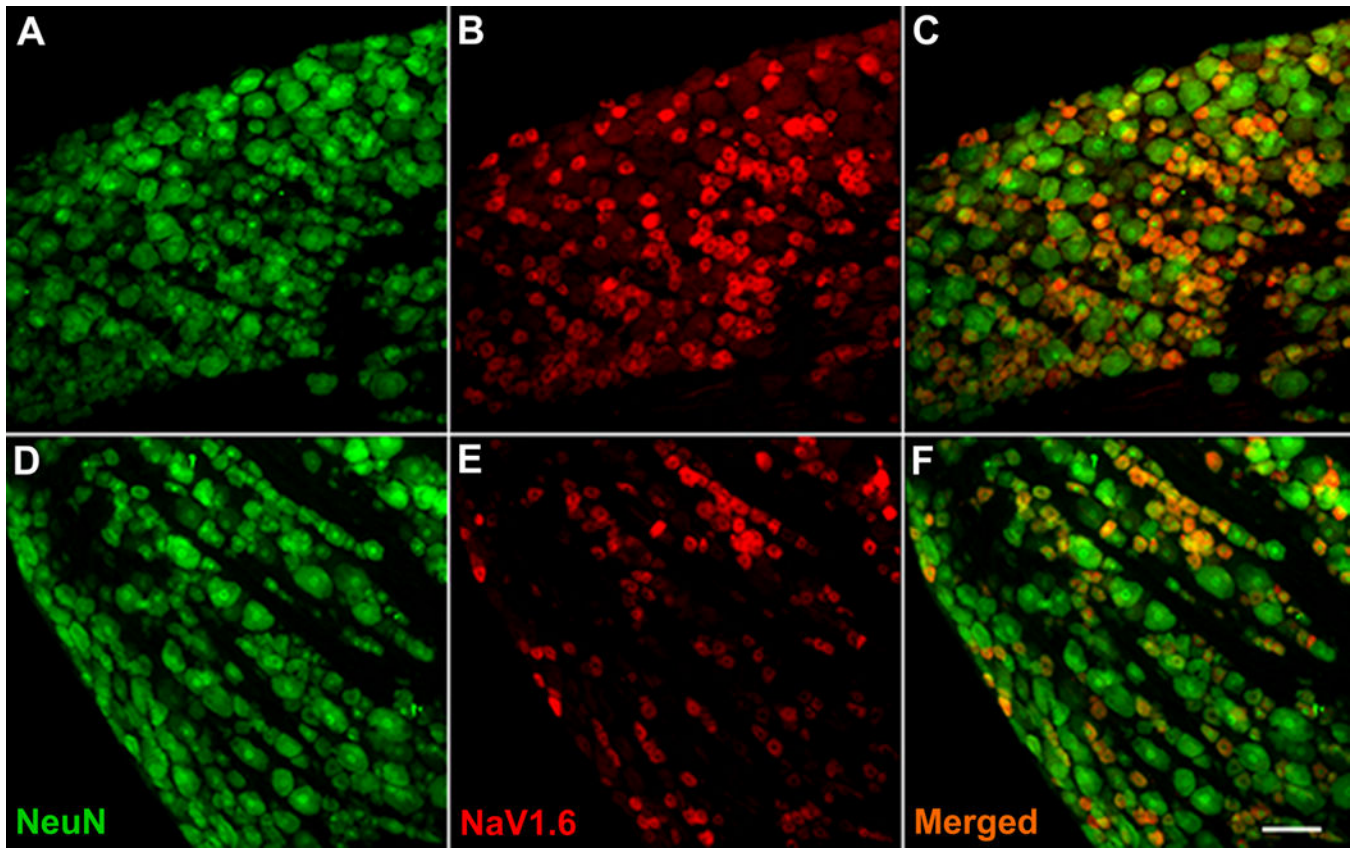
**Figure 2.** Immunohistochemical and Western blot detection of Navβ4. Sample sections stained for Navβ4 are shown from normal DRG (A), and DRG 4 days after DRG inflammation (“LID”) and injection of either Navβ4 (B) or nontargeting (“n.t.”) siRNA (C). Scale bar, 50 μm. D, summary data of Navβ4 intensity normalized to cellular area in DRG sections. \*\*, p<0.01; \*\*\*, p<0.001 significant difference between the indicated groups (one-way ANOVA with Tukey’s posttest). N = 4 animals per group, 19 to 34 sections per animal. Graph and statistical analysis are based on the animal averages. E, Summary data of the ratio of Navβ4 intensity to actin intensity from Western blot analysis of the same 3 experimental groups. Actin always appeared as a double band and both lanes were included in the actin measurement. \*, p<0.05, \*\*, p<0.01, significant difference between the indicated groups, one-way ANOVA with Tukey’s posttest. N = 6 samples per group. F, Two sample lanes from each experimental group. Some intervening lanes from a different experiment run on the same gel have been removed. Male and female animals were used for these experiments.



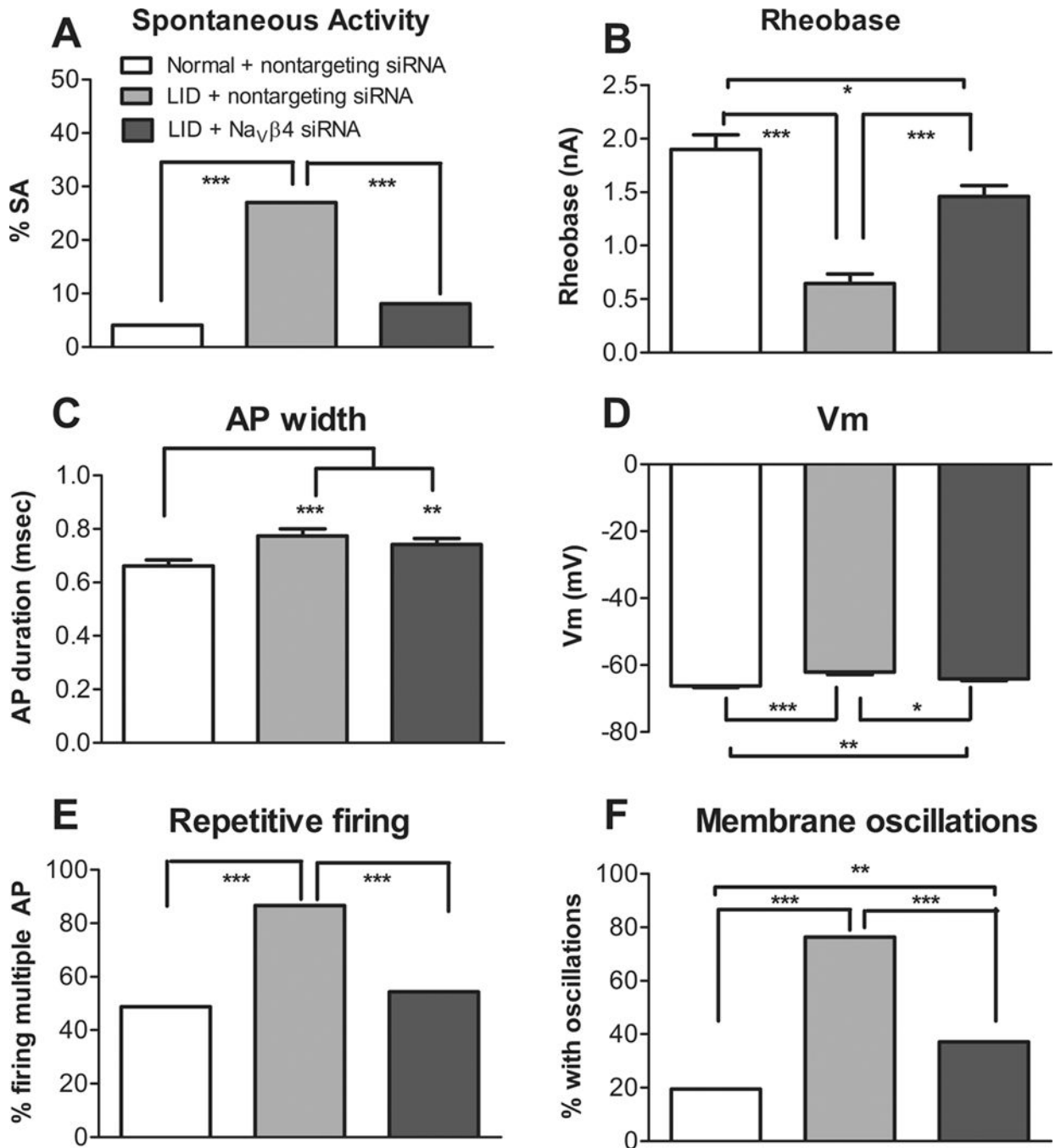
**Figure 3.**

$\text{Nav}\beta 4$  was preferentially expressed in larger cells both before and after DRG inflammation. DRG sections from normal and inflamed (“LID”) DRG 4 days after inflammation were stained for  $\text{Nav}\beta 4$  and all individual cells with nuclei in each section were scored as  $\text{Nav}\beta 4$ -positive or  $\text{Nav}\beta 4$ -negative and outlined for measurement of the cellular area. A, distribution histogram from normal DRG sections. B, distribution histogram from inflamed DRG. Note the lower incidence of  $\text{Nav}\beta 4$ -positive cells in the smallest bins in both conditions. C, Average area of  $\text{Nav}\beta 4$ -positive cells was significantly larger than that of  $\text{Nav}\beta 4$ -negative

cells under both conditions (\*\*\*,  $p < 0.001$ , ANOVA with Bonferroni's multiple comparison test), while the effect of condition was not significant in either  $\text{Nav}\beta 4$ -positive cells or  $\text{Nav}\beta 4$ -negative cells. Statistics were applied to the animal average values ( $n = 4$  rats per group; both sexes were used).



**Figure 4.** Effect of Nav $\beta$ 4 siRNA on immunohistochemical detection of Nav1.6 in DRG sections. Sample sections are shown from DRG 4 days after DRG inflammation and injection of either nontargeting siRNA (A, B, C) or Nav $\beta$ 4 siRNA (D, E, F). Scale bar, 100  $\mu$ m.

**Figure 5.**

Na<sub>v</sub>β4 knockdown reduces hyperexcitability of myelinated Aβ cells induced by DRG inflammation. L4/L5 DRGs were injected in vivo with either Na<sub>v</sub>β4 or nontargeting (“n.t.”) siRNA and inflamed (“LID”). For comparison normal DRGs were injected with nontargeting (“n.t.”) siRNA but not inflamed. Four days later DRGs were isolated for in vitro whole DRG microelectrode recording. Data are from myelinated Aβ cells based on dorsal root conduction velocity. A. Incidence of spontaneous activity was increased by LID and normalized by Na<sub>v</sub>β4 knockdown. B. Rheobase was reduced by LID and partially

normalized by  $\text{Na}_V\beta 4$  knockdown. C. Action potential duration was modestly increased by LID but not affected by  $\text{Na}_V\beta 4$  siRNA. D. Resting membrane potential was depolarized by LID and partially normalized by  $\text{Na}_V\beta 4$  siRNA. Responses to longer suprathreshold current injections showed that the percentage of cells that could be induced to fire repetitively (> 2 action potentials; E) or demonstrate subthreshold oscillations (F) was significantly increased by LID and partially normalized by  $\text{Na}_V\beta 4$  siRNA. \*,  $p < 0.05$ ; \*\*,  $p < 0.01$ ; \*\*\*,  $p < 0.001$ , significant difference between groups, Chi square test (A, E, F); Kruskal-Wallis test with Dunn's multiple comparison posttest (B, C,); ANOVA with Bonferroni's posttest (D). N = 123 normal + n.t. siRNA cells from 4 female rats, 74 LID + n.t. siRNA cells from 3 female rats, and 172 LID +  $\text{Na}_V\beta 4$  siRNA cells from 6 female rats.

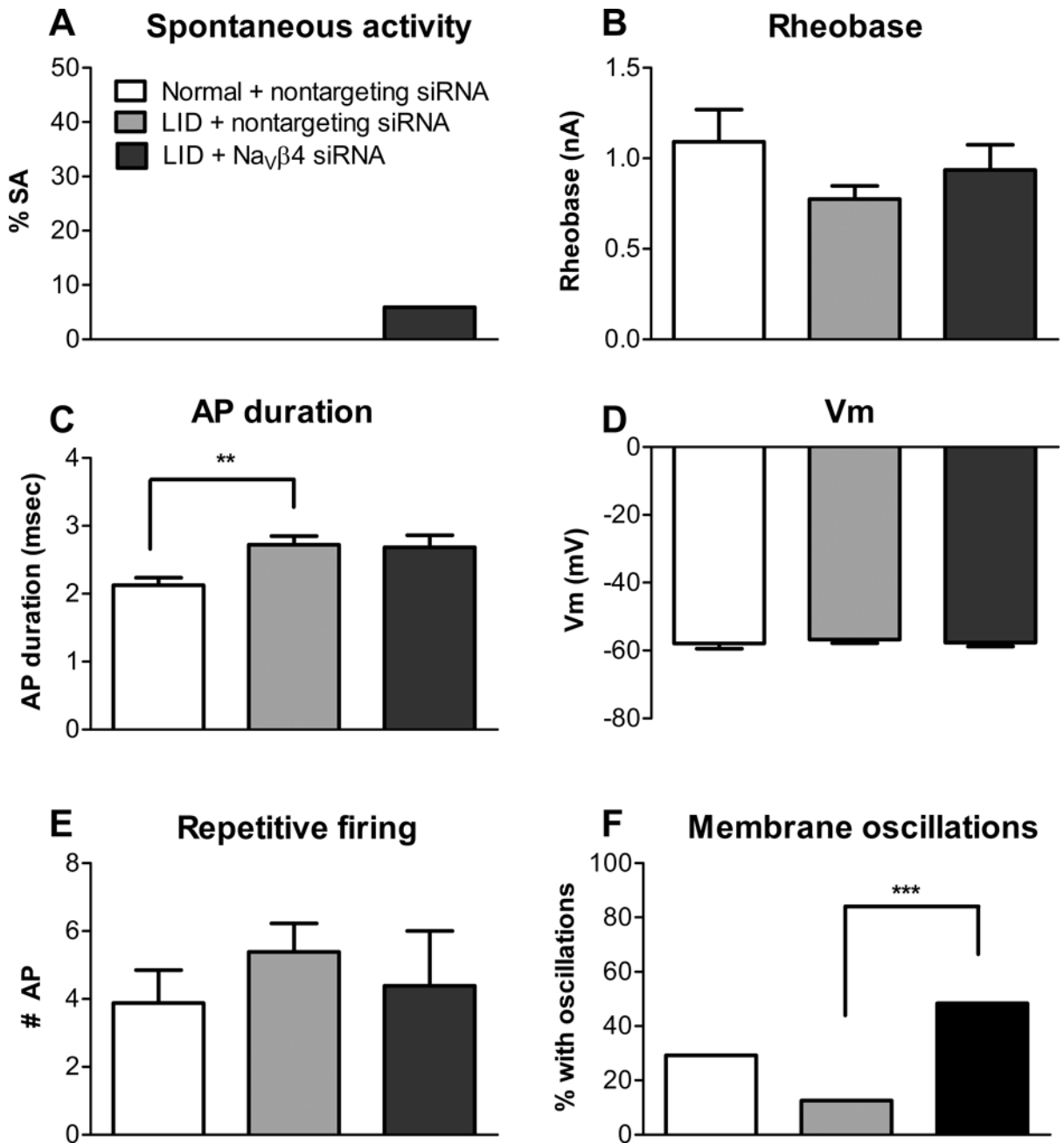


**Figure 6.**

DRG inflammation and Nav $\beta$ 4 knockdown have more modest effects in unmyelinated C cells. Data are from the same experiments and animals as Figure 5; data are from unmyelinated cells based on dorsal root conduction velocity. A. Incidence of spontaneous activity was zero except in the LID + Nav $\beta$ 4 group and did not differ significantly between groups (Chi Square test). B. Rheobase was not affected by LID or siRNA type (Kruskal-Wallis test,  $p = 0.44$ ). C. Action potential duration was modestly increased by LID. D. Resting membrane potential did not differ between groups (ANOVA with Bonferroni's multiple comparison test,  $p = 0.76$ ). Responses to longer suprathreshold current injections showed that the percentage of cells that could be induced to fire repetitively (E) did not

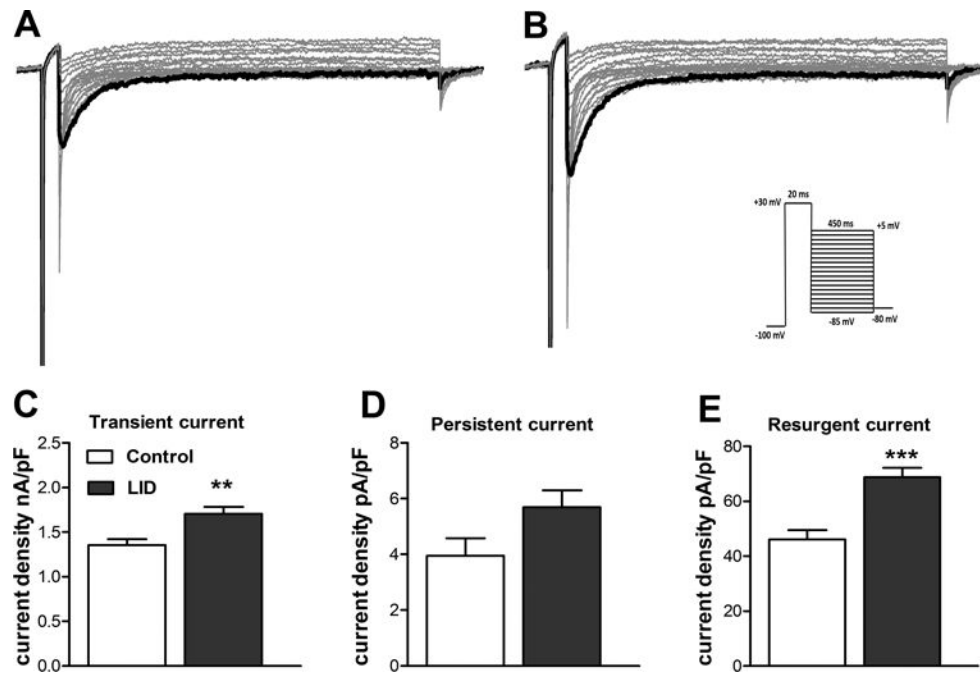
differ between groups (Chi Square test). F., In LID cells  $\text{Nav}\beta 4$  siRNA increased the percentage of cells able to demonstrate subthreshold oscillations. \*\*,  $p < 0.01$ ; \*\*\*,  $p < 0.001$ , significant difference between the indicated groups, Chi square test (F) or Kruskal-Wallis test with Dunn's multiple comparison posttest (C). N = 25 normal + n.t. siRNA cells, 50 LID + n.t. siRNA cells 34 LID +  $\text{Nav}\beta 4$  siRNA cells.

Author Manuscript

Author Manuscript

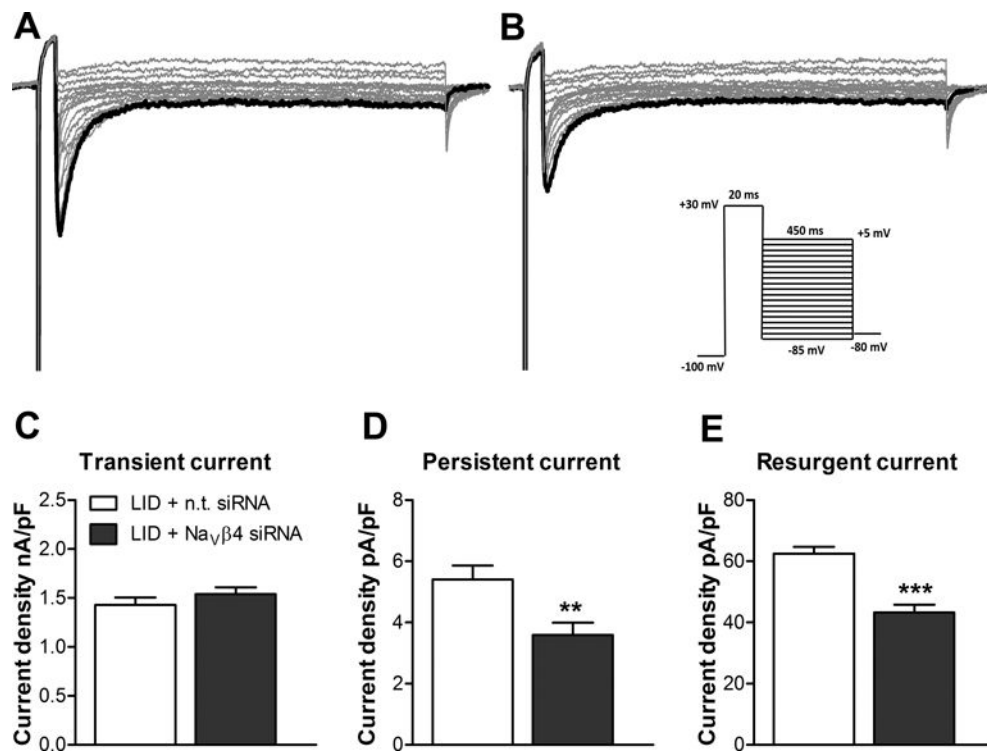
Author Manuscript

Author Manuscript



**Figure 7.**

TTX-sensitive resurgent and transient currents are increased by DRG inflammation. Na currents were recorded in acutely cultured medium diameter DRG neurons from control DRG (from sham operated animals) or from DRG 3 days after local DRG inflammation (“LID”). Data are from medium diameter cells that expressed only TTX-sensitive Na current. Sample traces are shown of resurgent current recordings from cells cultured from sham control (A) and inflamed (B) DRGs. The much larger transient current during the 20 mV pre-pulse (inset: voltage protocol) is off-scale. C – E: summary data shows both peak transient current (C) and resurgent current (E) densities were higher in cells from inflamed DRG ( $n = 15$  cells from 3 male rats) compared to sham control DRG ( $N = 20$  cells from 3 male rats). Increase in persistent current (D) did not reach significance ( $p = 0.055$ , Mann-Whitney test). \*\*,  $p < 0.01$ , \*\*\*,  $p < 0.001$ , significantly different from sham control (C, t-test; E, Mann-Whitney test).

**Figure 8.**

$\text{Na}_V\beta 4$  knockdown in vivo reduces TTX-sensitive persistent and resurgent currents in medium diameter neurons cultured from inflamed DRG. Na currents were recorded in acutely cultured medium diameter DRG neurons isolated from DRG 3 days after local DRG inflammation (“LID”) and injection of nontargeting (“n.t.”;  $N = 25$  cells from 5 male rats) or  $\text{Na}_V\beta 4$  siRNA ( $N = 31$  cells from 5 male rats). Data are from cells that expressed only TTX-sensitive current. Sample traces show resurgent current recordings from cells cultured from n.t. siRNA (A) and  $\text{Na}_V\beta 4$  siRNA (B) injected inflamed DRGs. The much larger transient current during the 20 mV pre-pulse (inset: voltage protocol) is off-scale. C – E: summary data shows both persistent current (D) and resurgent current (E) densities were reduced by  $\text{Na}_V\beta 4$  siRNA. \*\*,  $p < 0.01$ , \*\*\*,  $p < 0.001$ , significantly different from n.t. siRNA group (D, Mann-Whitney test; E, t-test).

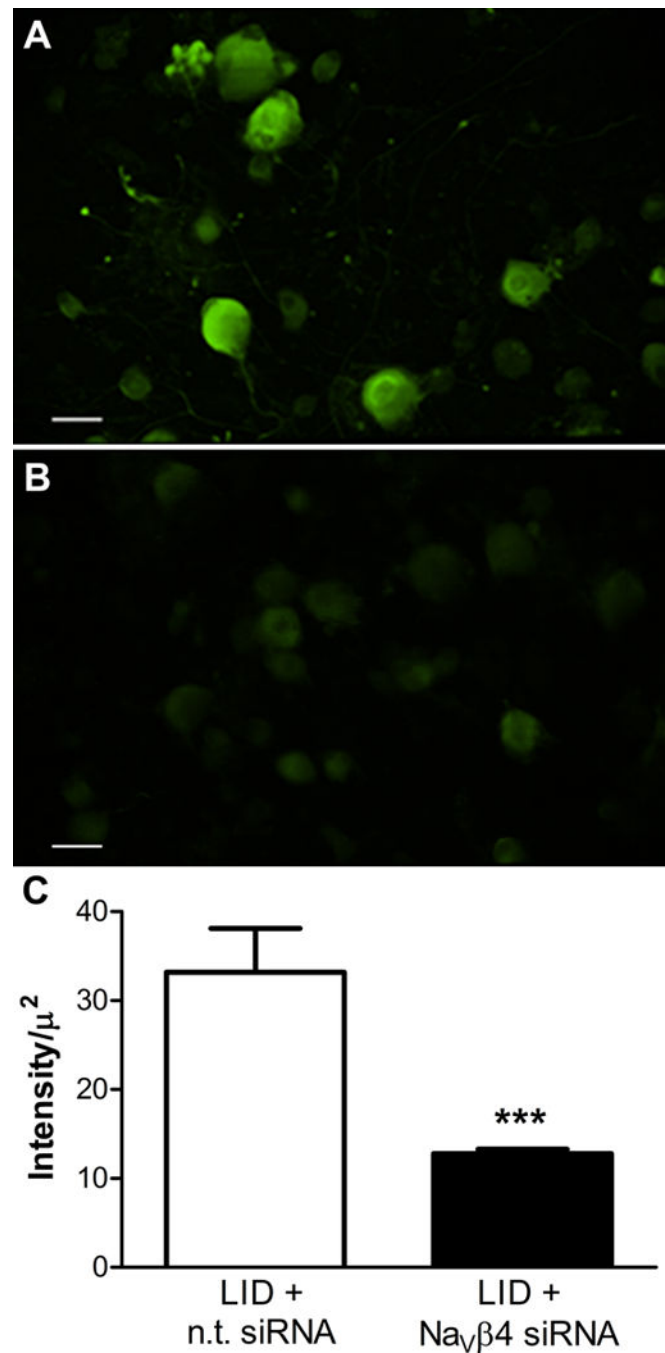


**Figure 9.** Immunohistochemical detection of  $\text{Nav}\beta 4$  in cultured DRG cells. Cells were obtained under the same conditions as for the electrophysiological experiments in Fig. 8: L4/L5 DRGs were injected in vivo with siRNA and inflamed (“LID”); 3 days later DRG neurons were isolated and cultured for 24 hours before fixation and staining for  $\text{Nav}\beta 4$ . A, sample image of cells from nontargeting (n.t.) siRNA injected DRG. B, Representative image of cells from  $\text{Nav}\beta 4$  siRNA injected DRG. Scale bars 50 $\mu\text{m}$ . C, Summary data of intensity per cell area from 1132 n.t. cells from 4 male rats and 1164  $\text{Nav}\beta 4$  cells from 3 male rats. \*\*\*, significant

difference between the groups ( $p < 0.001$ ), t test. Absolute intensity units are not comparable to Fig. 2 D because different microscopes and analysis programs were used.

Author Manuscript

Author Manuscript

Author Manuscript

Author Manuscript